JOURNAL OF MATERIALS SCIENCE 22 (1987) 2624–2628

Oxygen ionic conduction in Y_2O_3-stabilized Bi_2O_3 and ZrO_2 composites

M. MIYAYAMA, T. NISHI,* H. YANAGIDA
Department of Industrial Chemistry, Faculty of Engineering, University of Tokyo, 7-3-1 Hongo, Bunkyo-ku, Tokyo 113, Japan

Oxygen-ion conductivity was measured in two-phase mixed composites in the system fcc Bi_2O_3 (BY)–fcc ZrO_2 (ZY) stabilized with Y_2O_3 (Y = 20 at%). The composites appeared in the range $0.02 < x < 0.90$ for BY_xZY_{1-x} (mole fraction). Conductivity decreased with increasing ZY concentration. The composition dependence of conductivity could be explained by using an effective-medium approximation, although the conductivity was slightly higher than the calculated value in specimens containing ZY above 50 vol%.

1. Introduction

Among oxygen ion conductors, face-centred cubic Bi_2O_3 stabilized by doping of yttria or rare-earth oxides is known to show the highest conductivity. In a certain composition range, the conductivities of those stabilized Bi_2O_3 exceed 10^{-1} at 700° C and 10^{-2} ohm^{-1} cm^{-1} at 500° C [1–4]. Those values are one or two orders of magnitude higher than that of stabilized zirconia at corresponding temperatures.

The stabilized Bi_2O_3 has a deficient-fluorite structure, which has two vacant oxygen sites in a unit cell in pure fcc Bi_2O_3 [5]. The high ionic conductivity is attributed to the migration of oxygen ions through the vacancies [1].

In stabilized zirconia, oxygen ionic conduction is predominant (ionic transport number > 0.99) over a wide range of oxygen partial pressure ($P(O_2)$) down to about 10^{-15} Pa at 1000° C [6]. In contrast, stabilized Bi_2O_3 is easily reduced under low $P(O_2)$ and decomposed into bismuth metal at $P(O_2)$ of about 10^{-8} Pa at 600° C [7]. Accordingly, stabilized Bi_2O_3 is not suitable for practical use under very low $P(O_2)$ at high temperatures, such as in fuel cells. In addition, the mechanical strength of sintered specimens of Bi_2O_3-based materials is not high enough to fabricate complicated-shape devices.

The system of stabilized fcc Bi_2O_3 and fcc ZrO_2 is of interest in view of improvements in the above electrical and mechanical properties. Keizer *et al.* have investigated the phase diagram and electrical conductivity in the ZrO_2–Bi_2O_3–Y_2O_3 system [8–10]. However, because the melting points are markedly different for Bi_2O_3 (825° C) and ZrO_2 (≃2700° C), simultaneous sintering of the three components often gives inhomogeneous distribution of composition and, as a result, monoclinic ZrO_2 and tetragonal Bi_2O_3 are observed as second phases in most of the fcc phase.

In preliminary experiments, it was found that solid solutions and composites, consisting of fcc phases of Bi_2O_3 and ZrO_2, are obtained by using powders of fcc Bi_2O_3 and ZrO_2, both doped with Y_2O_3, as starting materials [11].

In the present paper, microstructure and electrical conductivity of the composites were investigated, and the observed conductivity was compared with values calculated using various mixing rules.

2. Experimental details

In the present system, yttrium concentration was kept constant at ~20.0%, i.e. $(Bi_2O_3)_{0.8}(Y_2O_3)_{0.2}$ (denoted as BY) and $(ZrO_2)_{0.889}(Y_2O_3)_{0.111}$ (ZY), respectively. Bi_2O_3 and Y_2O_3 were thoroughly mixed with ethanol and calcined in a platinum crucible. Two calcining (800, 870° C for 5 h), quenching and grinding procedures were carried out in order to prevent metastable second phases from forming. ZrO_2 and Y_2O_3 were mixed in PSZ ball mills, calcined in a platinum crucible at 1500° C for 5 h, and ground in PSZ ball mills for 6 h. Purities of starting materials were all 99.99%. Particle size distributions of the resulting powders were measured with a centrifugal particle size analyser.

Two kinds of powders were mixed in a desired ratio with ethanol, pressed into rectangular bars (5 mm × 5 mm × 15 mm) at 170 MPa, and sintered at 930° C for 12 h in air. For ZY-rich (> 50 mol% ZY) specimens with low sinterability, hot-pressing was performed at 900° C under 10 MPa for 6 h in air on pre-sintered (800° C) specimens.

The phases present in the samples were identified by X-ray diffraction measurements using Cu$K\alpha$ radiation. Lattice constants were calculated from more than six peak positions above 90° (2θ) by the least-square method using silicon as an internal standard.

The microstructure of the sintered samples was examined with the scanning electron microscope (SEM) and electron probe microanalysis (EPMA).

Alternating-current conductivity was measured in air at 350 to 800° C at frequencies of 5 Hz to 13 MHz using an r.f. impedance analyser. Platinum electrodes

Present address: Sekisui Plastics Co., Ltd, Central Laboratory, 670 Morimoto-cho, Tenri-shi, Nara 632, Japan.

0022–2461/87 $03.00 + .12

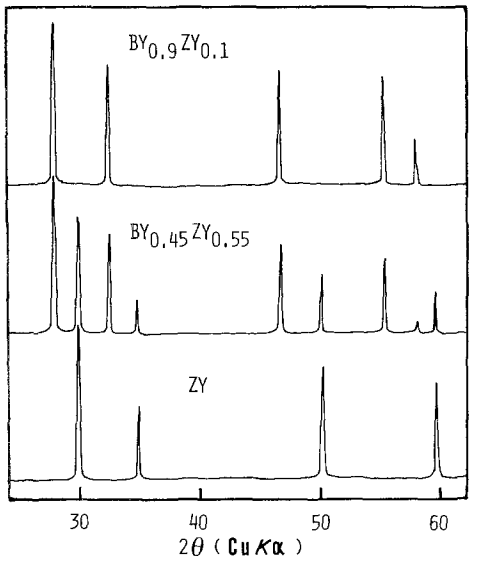

Figure 1 X-ray diffraction patterns of $BY_{0.9}ZY_{0.1}$, $BY_{0.45}ZY_{0.55}$ and ZY.

were applied by sputtering. For some samples, the dependence of conductivity on $P(O_2)$ was measured using Ar–O_2 mixed gas as a carrier gas and stabilized zirconia cells for reducing and monitoring the $P(O_2)$.

3. Results and discussion

More than 60% of powder particles before final sintering were 1 to 7 μm in size for BY and 1 to 5 μm for ZY, and average particle sizes were estimated to be 3.3 μm for BY and 2.2 μm for ZY, respectively.

Fig. 1 shows the X-ray diffraction patterns of the sintered specimens of $BY_{0.9}ZY_{0.1}$, $BY_{0.45}ZY_{0.55}$ (mole fraction), and ZY. Diffraction peaks of fcc BY and fcc ZY monophases were observed in the composition range $x \geqslant 0.90$ and $x \leqslant 0.02$ for BY_xZY_{1-x}, respectively. In the range of $0.02 < x < 0.90$, both BY and ZY peaks were observed as shown in Fig. 1, and there were no peaks of second phases other than the fcc phases.

In the monophasic region, the lattice constant of fcc BY decreased with increasing ZY concentration from 0.5506 nm (0 mol % ZY) to 0.5496 nm (10 mol % ZY), as reported elsewhere [11]. The lattice constant of fcc ZY increased on adding of BY from 0.5142 nm (0 mol % BY) to 0.5154 nm (2 mol % BY). In the two-phase region, the lattice constants of BY and ZY were almost constant. As a result, specimens BY_xZY_{1-x} in the composition range $0.02 < x < 0.90$ can be regarded as composites consisting of two fcc phases of $BY_{0.9}ZY_{0.1}$ (BY_{ss}) and $BY_{0.02}ZY_{0.98}$ (ZY_{ss}).

Porosities were 6 to 13% in normal-sintered specimens with $x > 0.6$ and 1 to 6% in hot-pressed specimens. Normal-sintering at high temperatures $> 1100°C$ also gave dense specimens even

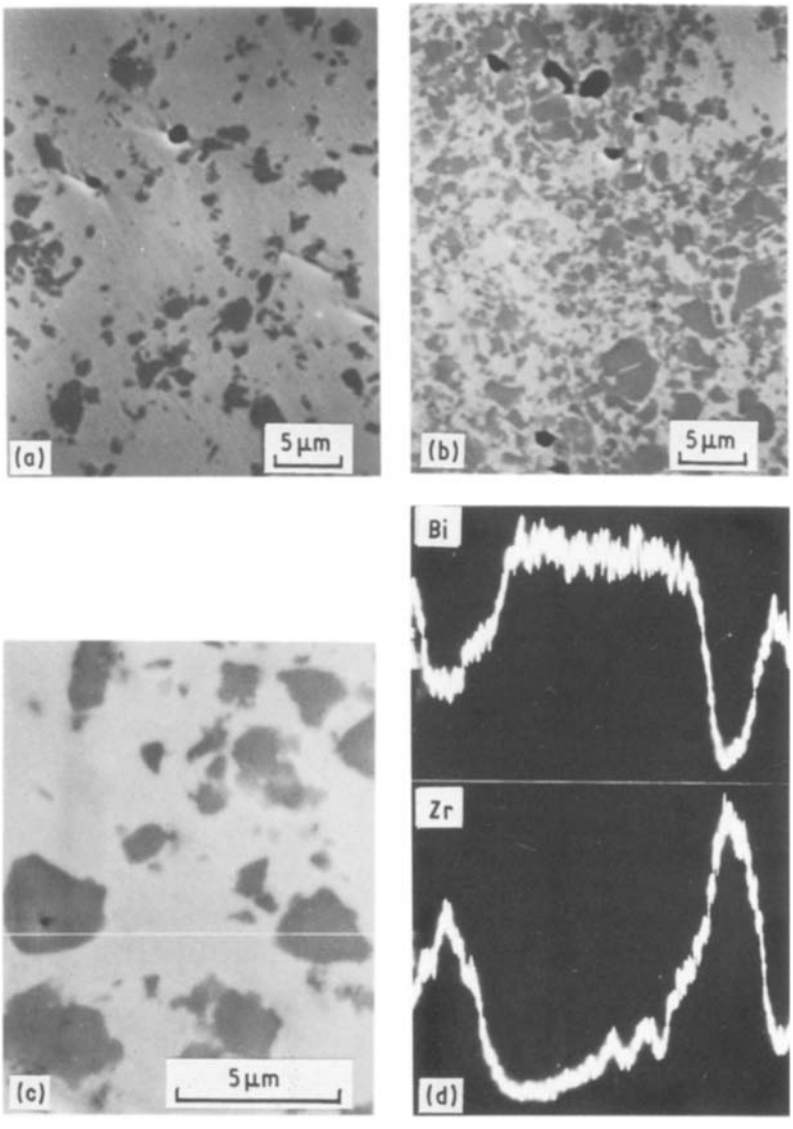

Figure 2 Scanning electron micrographs of polished surfaces of (a) $BY_{0.7}ZY_{0.3}$, (b) $BY_{0.2}ZY_{0.8}$ and (c) $BY_{0.45}ZY_{0.55}$, and (d) relative X-ray intensities of bismuth and zirconium on the line indicated in (c).

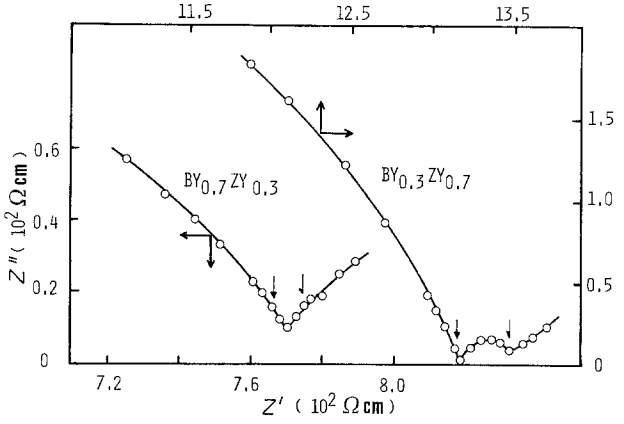

Figure 3 Typical impedance plots for $BY_{0.7}ZY_{0.3}$ and $BY_{0.3}ZY_{0.7}$ measured at 400° C; ⇀ and → indicate impedances at 1 and 100 kHz, respectively.

at $x > 0.5$, but tetragonal β-Bi_2O_3 appeared as a second phase.

Fig. 2 shows a polished surface of $BY_{0.7}ZY_{0.3}$ and $BY_{0.2}ZY_{0.8}$, and relative X-ray intensities of bismuth and zirconium. The dark particles are found to correspond to ZY_{ss}. The ZY_{ss} particles, 1 to 3 μm in size, were observed to be dispersed in BY_{ss} matrix. In monophasic specimens as $BY_{0.9}ZY_{0.1}$, bismuth, zirconium and yttrium atoms were distributed homogeneously.

As reported previously, the a.c. impedance of a polycrystalline ionic conductor such as stabilized zirconia contains contributions from the grains, the grain boundaries and the electrolyte/electrode impedance, and can be represented by three semicircles in the complex impedance plot [12, 13]. Fig. 3 shows typical impedance plots for $BY_{0.7}ZY_{0.3}$ and $BY_{0.3}ZY_{0.7}$ at 400° C. The low-frequency region (below 1 kHz) can be explained by the electrolyte/electrode impedance. Most of the impedance plots consisted of two sections of semicircles (grain and electrode impedance), as $BY_{0.7}ZY_{0.3}$. A small semicircle in the middle frequency region, which is assumed to be associated with a grain boundary, appeared only in the plots for specimens containing more than 40 mol% ZY below 500° C, as $BY_{0.3}ZY_{0.7}$ in Fig. 3. As the grain-boundary impedance can hardly be detected in Bi_2O_3-based materials, the second semicircle is assumed to be due to ZY/ZY grain boundaries. However, details are still unclear. Because the contribution of the grain-boundary impedance did not exceed 4% of the total impedance, the end-point of the first semicircle was taken as the resistance to calculate conductivity in the present study.

The temperature dependence of conductivity, σ, in typical specimens in the BY–ZY system is shown in Fig. 4. The conductivity of ZY was of a specimen sintered at 1500° C for 5 h. A bend in the Arrhenius plot (a change in activation energy) at about 550° C was observed in all specimens except for ZY solid solutions. This change in activation energy is generally observed in fcc Bi_2O_3 solid solutions with Y_2O_3 or Ln_2O_3 (Ln = Gd to Er) at low substituent concentrations, and is interpreted as a short-range order–disorder transformation in the oxygen sublattice [14]. The appearance of this change in activation energy indicates that there is no marked change of conduction mechanism in BY solid solutions and in individual BY_{ss} particles of the composites.

Fig. 5 shows the composition dependence of conductivity in the BY–ZY system. Both in the solid solution and the composite region, conductivity decreased as the ZY concentration increased.

The activation energy, E, and the pre-exponential term, σ_0, in the high (> 550° C) and low (< 550° C) temperature regions were calculated from

$$\sigma = \sigma_0 \exp(-E/kT) \quad (1)$$

where k and T have their usual meanings, and are presented in Fig. 6. In the solid solutions at $x \geqslant 0.9$ in BY_xZY_{1-x}, values of E and σ_0 in both temperature regions were almost in an agreement with reported data on fcc $(Bi_2O_3)_{0.8}(Ln_2O_3)_{0.2}$, and their composition dependences are also similar [3]. In the

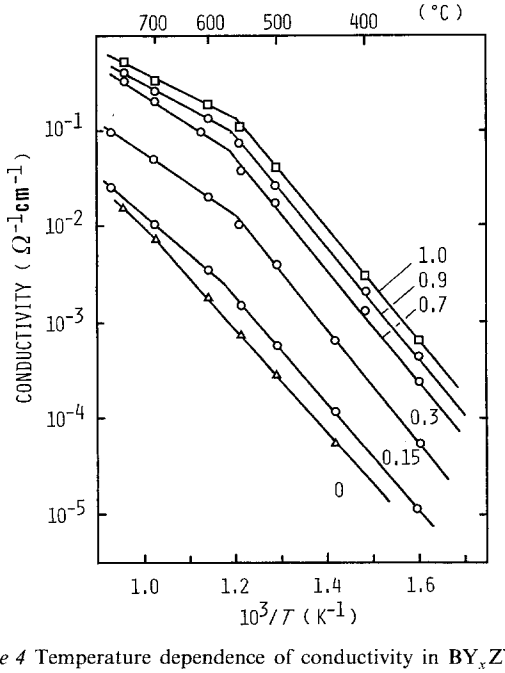

Figure 4 Temperature dependence of conductivity in BY_xZY_{1-x}. Numbers indicate x.

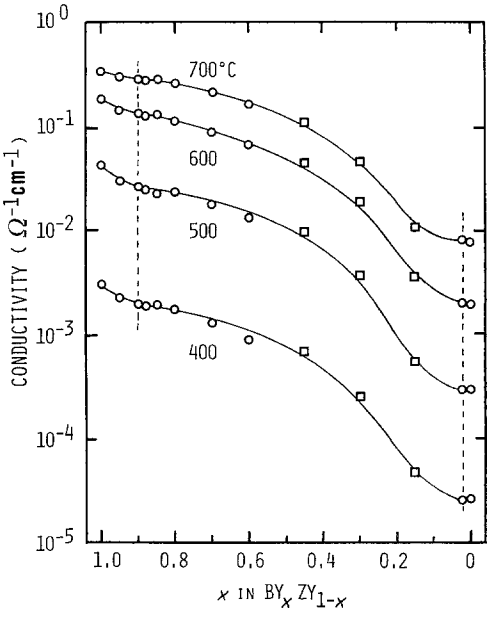

Figure 5 Composition dependence of conductivity in BY_xZY_{1-x} measured for (○) normal-sintered and (□) hot-pressed specimens. Dashed lines indicate solubility limits.

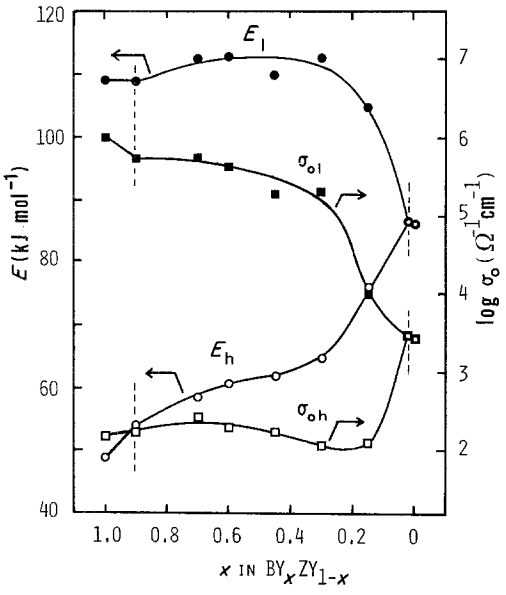

Figure 6 Activation energy, E, and preexponential term, σ_0, in BY_xZY_{1-x} in high (> 550° C) and low (< 550° C) temperature regions.

composites, E and σ_0 did not change very much with composition at $x > 0.3$ except for E at high temperatures. However, at $x < 0.3$, they rapidly approached the values of ZY_{ss} with increasing ZY concentration.

The dependence of conductivity on $P(O_2)$ for BY_xZY_{1-x} with $x = 0$, 0.1 and 0.4 at 800° C is shown in Fig. 7. The conductivities were kept constant under $P(O_2)$ between 10^5 and about 10^{-7} Pa, indicating oxygen conduction to be dominant. The conductivities decreased at $P(O_2)$ below 10^{-7} Pa. Specimens annealed at low $P(O_2)$ contained β-Bi_2O_3(ss), and bismuth metal was precipitated on the surface of the specimens. For the macroscopically homogeneous composites, as in the present study, the applicable $P(O_2)$ range for a solid electrolyte was confirmed to be determined by the dissociation $P(O_2)$ of the BY_{ss} component.

Numerous equations have been derived in an attempt to calculate the effective conductivity of heterogeneous materials, in general, for the two-phase system. Maxwell derived an expression for the effective conductivity of a solid consisting of spherical particles of one phase dispersed in a continuous matrix phase

$$\sigma = \sigma_1 \frac{\sigma_2 + 2\sigma_1 + 2V_2(\sigma_2 - \sigma_1)}{\sigma_2 + 2\sigma_1 - V_2(\sigma_2 - \sigma_1)} \quad (2)$$

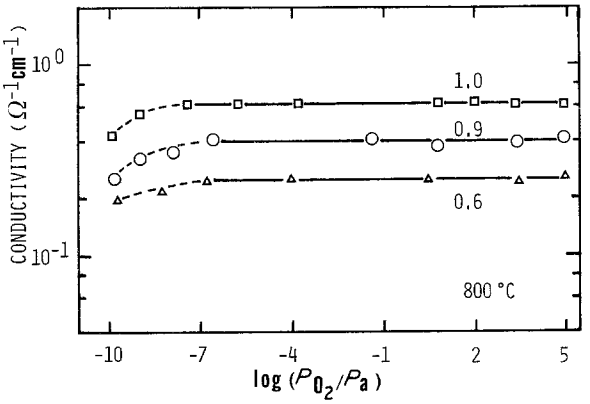

Figure 7 $P(O_2)$ dependence of conductivity in BY_xZY_{1-x}. Numbers

where subscript 1 refers to the matrix, subscript 2 to the dispersed phase, and V is the volume fraction [15]. Subsequently, this equation has extended to the more general case of ellipsoidal particles [16]. In these equations, it is generally assumed that the perturbation of the electric field around one particle does not influence the field around the other particles. This requires that the particles are well separated, and as a result the equations are applicable only up to a particle volume fraction $V_2 < 0.15$. This equation is often used for the porosity-correction of conductivity.

In order to expand the applicable region of volume fraction, the effective-medium theory was proposed originally by Bruggeman [17] and by Landauer [18] in a more formal manner. The effective-medium theory assumed that each additional particle is dispersed in a medium of some effective conductivity determined by the amount of dispersed phase already present. Landauer derived an equation in the case where there is no correlation between the positions of the two types of particle, as

$$\sigma = \tfrac{1}{4}\{(3V_1 - 1)\sigma_1 + (3V_2 - 1)\sigma_2 + [\{(3V_1 - 1)\sigma_1 + (3V_2 - 1)\sigma_2\}^2 + 8\sigma_1\sigma_2]^{1/2}\} \quad (3)$$

where subscripts 1 and 2 are the two types of phase.

Another method, percolation theory, can be used in the system consisting of conducting particles and insulating particles. An electrical current can flow through the system only when there is a completed path of adjacent conducting particles crossing the system. Kirkpatrick [19] and Pike *et al.* [20] calculated the effective conductivity of such random resistive networks statistically using Monte Carlo techniques. The conductivity is expressed as the following equation

$$\sigma(V) = A(V - V_c)^t \quad (4)$$

where V is the volume fraction of the conductive phase and V_c is the critical volume fraction able to make a completed conduction path and A and t are constants (t = 1.5 to 1.6).

Because of a practical dependence on the geometry and distribution of the individual components, attempts have been made to set upper and lower bounds on the properties of composite materials with arbitrary geometry. For the case of a macroscopically homogeneous and isotropic two-phase material, Hashin and Shtrikman [21] derived expressions for the upper and lower bounds of the effective conductivity, σ_u and σ_l as

$$\sigma_u = \sigma_B + \frac{V_A}{[1/(\sigma_A - \sigma_B)] + (V_B/3\sigma_B)} \quad (5)$$

$$\sigma_l = \sigma_A + \frac{V_B}{[1/(\sigma_B - \sigma_A)] + (V_A/3\sigma_A)} \quad (6)$$

where $\sigma_A < \sigma_B$. Although derived in an entirely independent manner, Equations 5 and 6 are the same with the Maxwell's Equation 2 for the two cases of component A dispersed in B (σ_u) and B in A (σ_l).

Fig. 8 shows conductivities at 500° C in the composite region ($0.02 < x < 0.9$) plotted against the

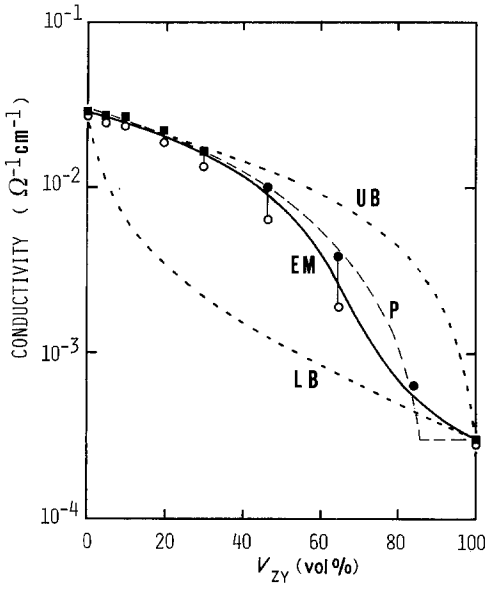

Figure 8 Conductivity in composites at 500° C plotted against volume fraction of ZY_{ss}; (○, ●) measured for normal-sintered and hot-pressed specimens, respectively, and (■) porosity-corrected. Lines UB and LB are calculated upper and lower bounds, EM by effective-medium theory, and P by percolation theory.

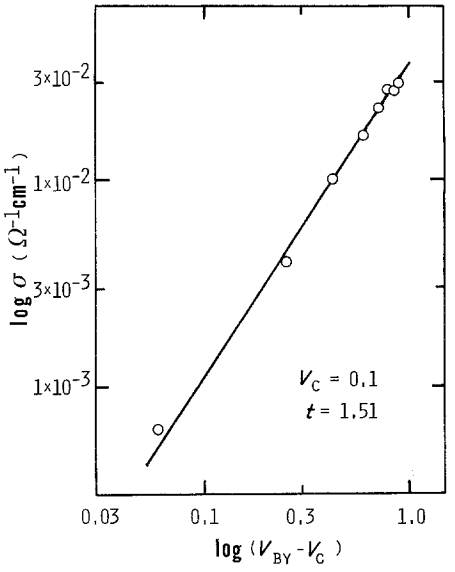

Figure 9 log σ–log ($V_{BY} - V_c$) plot at 500° C in composites for the case of $V_c = 0.1$.

volume fraction of ZY_{ss} (V_{ZY}). The volume fractions were calculated from the composition and unit-cell volumes of BY_{ss} and ZY_{ss}. In order to eliminate the porosity effect, a porosity correction was made on conductivity in normal-sintered specimens, using Maxwell's equation with $\sigma = 0$ for pores. In Fig. 8, calculated conductivities using Equations 2 to 6 are also presented for comparison.

The measured conductivities were situated between the upper and lower bounds calculated by Equations 5 and 6, and approximately agreed with the values of the effective-medium theory, suggesting that a correlation between the positions of the two kinds of particle is small. However, the measured values were a little higher than the calculated values in specimens with ZY > 50 vol %.

According to the percolation theory, log σ and log ($V - V_c$) should follow a linear relationship when the volume fraction, V, of conductive BY_{ss} phase is above a critical value V_c. Fig. 9 shows the log σ–log ($V_{BY} - V_c$) plot for the case $V_c = 0.1$. The plot gives a linear relation with a slope of 1.51. This suggests that the percolation theory can hold for the present system. The calculated conductivity, P, in Fig. 8 was that obtained by applying the tentative values $V_c = 0.1$, $t = 1.51$ and $A = 3.6 \times 10^{-2}$ into Equation 4.

The value of V_c (the minimum volume fraction for a completed conduction path) is reported to be dependent on the arrangement of particles, and has been calculated statistically to be 0.3 for single cubic and 0.2 for face-centred cubic lattice arrangements [19]. The value of V_c of 0.1 obtained in the present system is smaller than theoretical values. This suggests that conductive BY_{ss} particles are better-connected to form conduction paths than in the case of random distribution. On SEM observation (Fig. 2b), BY_{ss} appears to be better-connected than ZY_{ss} particles. Probably, the preferential arrangement of BY_{ss} is the cause of a little higher conductivity than that of effective-medium approximation. However, it is not clear whether this preferential arrangement is due to a low melting point of BY or to hot-pressing.

References

1. T. TAKAHASHI, H. IWAHARA and T. ARAO, *J. Appl. Electrochem.* **5** (1975) 187.
2. H. T. CAHEN, T. G. M. VAN DEN BELT, J. H. W. De WIT and G. H. J. BROERS, *Solid State Ionics* **1** (1980) 411.
3. M. J. VERKERK and A. J. BURGGRAAF, *J. Electrochem. Soc.* **128** (1981) 75.
4. H. IWAHARA, T. ESAKA, T. SATO and T. TAKAHASHI, *J. Solid State Chem.* **39** (1981) 173.
5. H. A. HARWIG, *Z. Anorg. Allg. Chem.* **444** (1978) 151.
6. T. H. ETSELL and S. N. FLENGAS, *J. Electrochem. Soc.* **119** (1972) 1.
7. T. TAKAHASHI, T. ESAKA and H. IWAHARA, *J. Appl. Electrochem.* **7** (1977) 303.
8. K. KEIZER, M. J. VERKERK and A. J. BURGGRAAF, *Ceram. Int.* **5** (1979) 143.
9. K. KEIZER, A. J. BURGGRAAF and G. De WITH, *J. Mater. Sci.* **17** (1982) 1095.
10. A. J. A. WINNUBST and A. J. BURGGRAAF, *Mater. Res. Bull.* **19** (1984) 613.
11. M. MIYAYAMA and H. YANAGIDA, *ibid.* **21** (1986) 1215.
12. J. E. BAUERLE, *J. Phys. Chem. Solids* **30** (1969) 2657.
13. M. MIYAYAMA, H. INOUE and H. YANAGIDA, *J. Amer. Ceram. Soc.* **66** (1983) c-164.
14. M. J. VERKERK, G. M. H. VAN De VELDE, A. J. BURGGRAAF and R. B. HELMHOLDT, *J. Phys. Chem. Solids* **43** (1982) 1129.
15. J. C. MAXWELL, in "Treatise on Electricity and Magnetism, Vol. 1" 3rd Edn (Clarendon, London, 1892).
16. H. FRICKE, *J. Phys. Chem.* **57** (1953) 934.
17. D. A. G. BRUGGEMAN, *Ann. Phys. (Leipzig)* **24** (1935) 636.
18. R. LANDAUER, *J. Appl. Phys.* **23** (1952) 779.
19. S. KIRKPATRICK, *Rev. Mod. Phys.* **45** (1973) 574.
20. G. E. PIKE, W. J. CAMP, C. H. SEAGER and G. L. McVAY, *Phys. Rev. B* **10** (1974) 4909.
21. Z. HASHIN and S. SHTRIKMAN, *J. Appl. Phys.* **33** (1962) 3125.

Received 4 September
and accepted 12 November 1986